Original Article
pISSN 1738-2637 / eISSN 2288-2928
J Korean Soc Radiol 2017;77(3):148-156
https://doi.org/10.3348/jksr.2017.77.3.148

대한영상의학회지

Alterations of White Matter Integrity in Patients with Chronic Obstructive Pulmonary Disease: Tract-Based Analysis Using TRActs Constrained by UnderLying Anatomy

만성 폐쇄성 폐질환에서 백색질다발통합성 변화: TRActs Constrained by UnderLying Anatomy를 이용한 신경다발 분석

Mi-Kyung Um, MD[1], Seung-Hwan Lee, MD[2,3], Woo Jin Kim, MD[4,5], Seong Whi Cho, MD[1], Hye-Kyung Yoon, MD[1], Myoung-nam Lim, PhD[5], Sung-Bom Pyun, MD[6,7], Woo-Suk Tae, PhD[3,6], Sam-Soo Kim, MD[1,3]*

Departments of [1]Radiology, [2]Neurology, [4]Internal Medicine, Kangwon National University Hospital, Kangwon National University School of Medicine, Chuncheon, Korea
[3]Neuroscience Research Institute, [5]Environmental Health Center, Kangwon National University Hospital, Kangwon National University School of Medicine, Chuncheon, Korea
[6]Brain Convergence Research Center, [7]Department of Physical Medicine and Rehabilitation, Korea University Anam Hospital, Korea University College of Medicine, Seoul, Korea

Purpose: To investigate structural brain changes and their relationship with cognitive function by determining the alterations of white matter integrity and changes in hippocampal volume that occur during chronic obstructive pulmonary disease (COPD).
Materials and Methods: Diffusion tensor images and 3D-T1 MR images were acquired in 13 male nonhypoxemic COPD patients and 13 age- and gender-matched healthy controls. Global probabilistic tractography was used to assess a total of 18 major tracts. We examined the association between the hippocampal volume and diffusivity parameters of white matter tracts.
Results: A significant difference in diffusion parameters between groups was identified for 11 white matter bundles ($p < 0.05$). No association was demonstrated between the normalized hippocampus volume and diffusion parameters among the participants. Significant associations between Korean version of the Mini-Mental State Examination (K-MMSE) scores and diffusivities were found for six tracts ($p < 0.05$). Of note, the mean diffusivity (MD) and redial diffusivity (RD) of the left superior longitudinal fasciculus parietal segment showed a significant negative correlation with the K-MMSE score (MD: $r = -0.623$, $p = 0.001$; RD: $r = -0.408$, $p = 0.048$).
Conclusion: Altered white matter integrity was demonstrated across regional white matter bundles, including the superior longitudinal fasciculus, in COPD patients, and it was related to cognitive function. Changes in the volume of the hippocampus should be investigated in further studies.

Index terms
Diffusion Tensor Imaging
White Matter
Chronic Obstructive Pulmonary Disease

Received January 3, 2017
Revised January 15, 2017
Accepted January 26, 2017
***Corresponding author:** Sam-Soo Kim, MD
Department of Radiology, Kangwon National University Hospital, Kangwon National University School of Medicine, 156 Baengnyeong-ro, Chuncheon 24289, Korea.
Tel. 82-33-258-2489 Fax. 82-33-258-2221
E-mail: samskim@kangwon.ac.kr

INTRODUCTION

Chronic obstructive pulmonary disease (COPD) is a leading cause of morbidity and mortality, and it is considered a multisystemic disease that includes brain pathology (1, 2). Hypoxemia resulting from irreversible airflow limitation and neuronal damage caused by systemic inflammation leads to structural brain damage (3). Many studies have investigated structural brain damage or dysfunction in COPD patients. Several studies have suggested regional structural brain changes in COPD patients (4,

5). Dodd et al. (4) reported that white matter integrity is reduced in COPD patients, which is independent of smoking and cerebrovascular comorbidity, but the mechanisms remain unclear.

Magnetic resonance imaging (MRI) has been used for the evaluation of structural brain changes. While providing anatomical information on the brain, conventional MRI techniques have limitations in spatial resolution and contrast that do not allow demonstration of microstructural damage (6). Diffusion tensor imaging (DTI) enables visualization and characterization of white matter bundles through diffusion MRI measurements (7, 8). DTI parameters include fractional anisotropy (FA), which provides a measure of tissue structural integrity, and mean diffusivity (MD), which reflects the tissue microstructure.

TRActs Constrained by UnderLying Anatomy (TRACULA) is an automated probabilistic reconstruction of a set of major white matter pathways from diffusion-weighted MR images. It utilizes prior information on the anatomy of the pathways from a set of training subjects (1) and provides information on the specific tract involved in a disease and the type of damage. The robustness of TRACULA has been validated in prior studies, which have shown meaningful results (1, 9-15).

Cognitive impairment is an important extrapulmonary manifestation in COPD patients (16, 17). However, it has not been fully determined whether structural brain changes are associated with cognitive dysfunction in COPD patients. Some studies using neuroimaging have found that adults with severe COPD may develop alterations in brain perfusion as a result of hypoxemia, and this change has been hypothesized to affect cognitive performance and cause cognitive impairment (18). The hippocampus plays a critical role in cognitive function (19) and it is particularly vulnerable to hypoxemia (20). A pattern of cognitive dysfunction specific to COPD may exist (17). Therefore, the question arises as to whether detectable changes in the volume of the hippocampus occur in COPD patients.

The purpose of this study was to investigate alterations in the microstructural integrity of the white matter and the volume of the hippocampus in stable nonhypoxemic COPD patients compared to those in age- and gender-matched control subjects. We hypothesized that TRACULA would detect altered white matter integrity in COPD patients versus control subjects, and the alteration of white matter integrity would be associated with structural changes in the hippocampus.

MATERIALS AND METHODS

Participants

This prospective study was approved by our institution's research Ethics Board, and written informed consent was obtained from all patients. Stable nonhypoxemic male COPD patients between 50 to 80 years of age who had not experienced any exacerbations for 8 weeks at the time of data collection were recruited from our outpatient respiratory clinic in 2013. The patients were clinically diagnosed according to the diagnostic criteria of the Global Initiative for Chronic Obstructive Lung Disease [GOLD; post-bronchodilator forced expiratory volume 1/forced vital capacity (FEV_1/FVC) < 0.7] and categorized according to the GOLD criteria. Patients were excluded if they had a history of any other pulmonary disease, cerebrovascular disease, brain trauma, psychiatric disorders, or any other neurological or medical conditions that could result in cognitive changes. All patients underwent pulmonary function tests. Sixteen COPD patients were recruited, and three patients withdrew from the study because they decided to discontinue their participation before image acquisition. A total of 13 male, stable, nonhypoxemic patients (age 66.0 years, IQR 63.0–67.0) with COPD were included. Age- and gender-matched control participants were recruited from our respiratory and neurology outpatient clinics. A history of COPD was an exclusionary criterion for control participants, and the other exclusion criteria were the same as in the patient group. Thirteen male participants (age 66.0 years, IQR 58.1–71.0) were enrolled in the control group. The Korean version of the Mini-Mental State Examination (K-MMSE) was used to evaluate general cognitive functions.

MRI Acquisition

DTI and three-dimensional (3D) T1 MRIs were acquired with a 3.0 T Achieva (Philips Medical Systems, Best, the Netherlands) MRI system. A 3D structural MRI was acquired using a T1-weighted turbo field echo sequence [repetition time/echo time (TR/TE) = 9.9 ms/4.6 ms, field of view (FOV) = 240 × 240 × 195 mm^3, matrix = 256 × 256, number of excitations (NEX) = 1, slice thickness = 1.0 mm]. A DTI pulse sequence with single shot diffusion-weighted echo planar imaging (TR/TE = 8380 ms/94 ms, FOV = 224 × 224 × 130 mm^3, matrix = 112 × 110, NEX = 1, slice thickness = 2.0 mm) was applied in 32 directions (b-value

= 1000 s/mm^2). At the time of MRI acquisition, two experts performed visual scans to determine whether participants had gross brain abnormalities and to evaluate the adequacy of the data for fiber reconstruction.

Imaging Processing

Eighteen major fiber bundles were constructed by TRACULA, which is part of the FreeSurfer module (1, 21). TRACULA is a method for automatic reconstruction of a set of major white matter pathways from diffusion-weighted MRIs. It uses global probabilistic tractography with prior anatomical information from a set of 18 manually labeled tracts (1).

The acquired 32-direction DTI data were preprocessed to correct for head motion and distortions induced by eddy current by aligning the diffusion-weighted images to non-diffusion-weighted b = 0 images. The b = 0 images were registered to the same subject's T1-weighted images using a registration method that seeks to maximize the intensity contrast of the b = 0 image across the cortical gray/white boundary (22). Each subject's own T1-weighted image was registered to the 1 mm-resolution MNI-152 atlas (23) by applying affine registration (24). Using FreeSurfer 5.3 (http://surfer.nmr.mgh.harvard.edu), cortical parcellations and subcortical segmentations were generated from each individual's 3D T1 MR images (25-29).

Using FSL's DTIFIT, which fits a diffusion tensor model at each voxel of the DTI gradient data (http://www.fmrib.ox.ac.uk/fsl), FA, MD, axial diffusivity (AD), and radial diffusivity (RD) were calculated and images showing these measures were generated. FSL's bedpostX applied the ball-and stick model of diffusion to attain the participant's local diffusion orientations (30). TRACULA uses each subject's ball-and-stick model of local diffusion orientations and the labels of the same subject's cortical and subcortical segmentation. The volumetric distributions of the 18 major white matter pathways were reconstructed by combining them with prior information on each tract's position relative to these labels. Then, the tensor-based measures (FA, AD, RD, and MD) for the reconstructed pathways were separately extracted. The 18 reconstructed white matter pathways included the corpus callosum-forceps major (FMAJ) and corpus callosum-forceps minor (FMIN) in the corpus callosum, inferior longitudinal fasciculus (ILF), superior longitudinal fasciculus-parietal endings (SLFP), superior longitudinal fasciculus-temporal endings (SLFT), corticospinal tract, uncinate fasciculus (UF), anterior thalamic radiation, cingulum-cingulate gyrus bundle (CCG), and cingulum-angular bundle (CAB). The intracranial volume (ICV), which was measured manually, was used to normalize the hippocampal volume [(sum of both hippocampus volumes divided by the ICV) ×100] (31).

Statistical Analyses

Statistical analyses were performed using SAS ver. 9.4 (SAS Institute Inc., Cary, NC, USA). A non-parametric Mann-Whitney U-test was used to analyze age, K-MMSE scores, ICV, and normalized hippocampal volume. Diffusion parameters (FA, AD, MD, and RD) were extracted for each of the reconstructed pathways. A group difference in the diffusion parameters was found using ranked ANCOVA.

We analyzed the partial correlation between normalized hippocampal volume and DTI parameters of white matter bundles with age and ICV as covariates using the Spearman partial correlation. Correlations between K-MMSE scores and diffusion parameters were also analyzed.

RESULTS

Demographic data are summarized in Table 1. No significant differences were found in age, ICV, and normalized hippocampal volume between the controls and COPD patients. COPD patients did not exhibit significant hypoxemia (SpO2 = 96 ± 1.88%). K-MMSE scores were significantly lower in the COPD group (p = 0.010). The 18 reconstructed tracts used in the data set are shown in Fig. 1.

Significant group differences in DTI parameters were identified using ranked ANCOVA for the FMAJ (FA: p = 0.012, RD: p = 0.013), FMIN (MD: p = 0.047, RD: p = 0.047), left ILF (FA: p = 0.023, AD: p = 0.047), right ILF (FA: p = 0.008, RD: p = 0.018), left SLFP (FA: p = 0.047, MD: p = 0.005, RD: p = 0.035), right SLFP (AD: p = 0.038), left SLFT (MD: p = 0.035), left UF (AD: p = 0.007), right UF (FA: p = 0.023, RD: p = 0.042), left CAB (MD: p = 0.007, AD: p = 0.011, RD: p = 0.035), and right CAB (MD: p = 0.017, RD: p = 0.005), as shown in Table 2.

Table 3 shows the association between diffusion parameters and normalized hippocampus volume and the association between diffusion parameters and K-MMSE scores. No associa-

Table 1. Demographic Information, K-MMSE Scores, ICV, and Hippocampal Volume of Controls and COPD Participants

	Control	COPD	*p*-Value
Number	13	13	-
Gender	M	M	-
Age*	66.0 (63.0–67.0)	66.0 (58.0–71.0)	0.35
K-MMSE*	28.0 (28.0–29.0)	27.0 (26.0–28.0)	0.01
SpO2 (%)	-	96 ± 1.88	-
Post FEV_1 (%)	-	57.15 ± 20.77	-
ICV (cm^3)*	1559069.82 (1530193.36–1623814.45)	1528650.54 (1451825.68–1602984.38)	0.22
Normalized hippocampus volume (%)*	0.38 (0.36–0.39)	0.39 (0.38–0.40)	0.15

*Median (IQR) using a Mann-Whitney U-test.
COPD = chronic obstructive pulmonary disease, FEV_1=forced expiratory volume 1, ICV = intracranial volume, K-MMSE = Korean version of the Mini-Mental State Examination

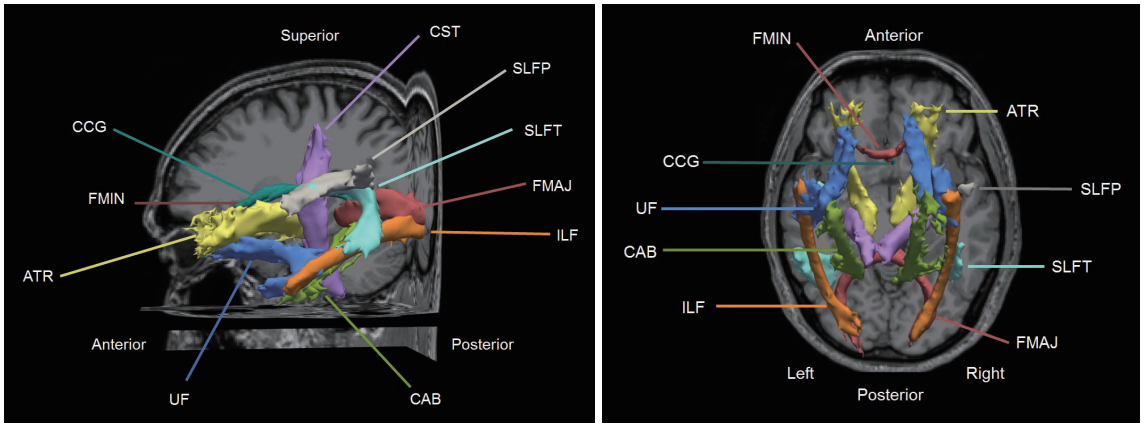

A B

Fig. 1. Eighteen automatically reconstructed white matter tracts from TRACULA [sagittal **(A)** and axial projective view **(B)**].
ATR = anterior thalamic radiation, CAB = cingulum-angular bundle, CCG = cingulum-cingulate gyrus bundle, CST = corticospinal tract, FMAJ = corpus callosum-forceps major, FMIN = corpus callosum-forceps minor, ILF = inferior longitudinal fasciculus, SLFP = superior longitudinal fasciculus-parietal endings, SLFT = superior longitudinal fasciculus-temporal endings, TRACULA = TRActs Constrained by UnderLying Anatomy, UF = uncinate fasciculus

tion was demonstrated between the normalized hippocampus volume and DTI parameters among the participants. Significant associations between K-MMSE scores and diffusivities were found for several tracts, including the left SLFP (MD: $p = 0.001$, RD: $p = 0.048$), left SLFT (AD: $p = 0.006$), right SLFT (AD: $p = 0.032$), and left CCG (AD: $p = 0.014$). Of note, the MD and RD of the left SLFP showed a significant negative correlation with the K-MMSE score (MD: $r = -0.623$, $p = 0.001$; RD: $r = -0.408$, $p = 0.048$).

DISCUSSION

COPD is a leading cause of morbidity and mortality and it has been recognized as a multi-component disease. Cognitive impairment is a significant extrapulmonary manifestation that is associated with increased mortality and disability in COPD patients (16, 17). A major mechanism proposed for cognitive decline in COPD patients is the neuronal damage mediated through hypoxia (17). However, the mechanism of cognitive dysfunction is unclear (17).

Diffuse white matter changes in COPD patients have been noted in conventional MR images. Recent advances in neuroimaging technology allow for a finer description of structural brain changes. DTI plays a critical role in the study of diseases that affect the brain, which allows prediction of the integrity of white matter tracts (4). TRACULA is an automated probabilistic reconstruction of a set of major white matter pathways from diffusion-weighted MR images. This technique provides information on the specific tract involved in a disease and the type of damage (1). This study is one of the first studies to investigate

Table 2. Median (IQR) of Diffusion Parameters in Controls and COPD Participants

DPI Parameters	Left Hemisphere			Right Hemisphere		
	Control	COPD	*p*-Value	Control	COPD	*p*-Value
	Forceps major			Forceps minor		
FA	0.79 (0.73–0.86)	0.72 (0.70–0.74)	0.012*	0.77 (0.74–0.78)	0.67 (0.59–0.72)	0.052
MD (× 10^{-4})	4.14 (4.07–4.29)	4.28 (4.09–4.44)	0.196	4.17 (4.04–4.27)	4.64 (4.38–5.42)	0.047*
AD (× 10^{-3})	1.05 (0.97–1.08)	0.96 (0.93–1.05)	0.052	0.91 (0.90–0.94)	0.90 (0.85–0.94)	0.256
RD (× 10^{-4})	1.14 (0.84–1.48)	1.72 (1.58–2.04)	0.013*	1.63 (1.44–1.80)	2.55 (2.05–3.56)	0.047*
Inferior longitudinal fasciculus						
FA	0.77 (0.74–0.78)	0.74 (0.70–0.76)	0.023*	0.73 (0.73–0.76)	0.70 (0.69–0.73)	0.008*
MD (× 10^{-4})	4.15 (0.47–4.25)	4.03 (3.98–4.33)	0.420	4.19 (4.06–4.27)	4.18 (4.02–4.41)	0.361
AD (× 10^{-3})	0.88 (0.85–0.90)	0.84 (0.84–0.86)	0.047*	0.84 (0.83–0.87)	0.83 (0.82–0.86)	0.146
RD (× 10^{-4})	1.81 (1.72–2.00)	2.00 (1.79–2.12)	0.068	1.93 (1.86–2.08)	2.20 (2.03–2.27)	0.018*
Superior longitudinal fasciculus (parietal segment)						
FA	0.70 (0.68–0.73)	0.68 (0.62–0.71)	0.047*	0.69 (0.66–0.72)	0.68 (0.64–0.69)	0.135
MD (× 10^{-4})	3.76 (3.64–3.86)	3.97 (3.82–4.16)	0.005*	3.74 (3.67–3.98)	3.90 (3.83–4.08)	0.062
AD (× 10^{-3})	0.74 (0.70–0.77)	0.74 (0.73–0.75)	0.157	0.72 (0.71–0.74)	0.73 (0.73–0.75)	0.038*
RD (× 10^{-4})	2.02 (1.88–2.17)	2.21 (2.04–2.57)	0.035*	2.07 (1.91–2.18)	2.18 (2.10–2.41)	0.068
Superior longitudinal fasciculus (temporal segment-arcuate)						
FA	0.74 (0.72–0.76)	0.74 (0.69–0.75)	0.196	0.70 (0.67–0.72)	0.70 (0.68–0.72)	0.480
MD (× 10^{-4})	3.78 (3.74–3.84)	3.88 (3.83–4.03)	0.035*	3.79 (3.72–4.01)	3.87 (3.79–4.04)	0.196
AD (× 10^{-3})	0.78 (0.76–0.79)	0.78 (0.77–0.79)	0.097	0.76 (0.73–0.77)	0.76 (0.75–0.78)	0.135
RD (× 10^{-4})	1.82 (1.68–1.94)	1.89 (1.81–2.18)	0.125	2.02 (1.94–2.10)	2.02 (1.95–2.12)	0.420
Corticospinal tract						
FA	0.82 (0.79–0.83)	0.82 (0.81–0.83)	0.480	0.80 (0.79–0.82)	0.81 (0.79–0.82)	0.272
MD (× 10^{-4})	3.73 (3.67–3.86)	3.69 (3.63–3.76)	0.240	3.79 (3.74–3.89)	3.78 (3.68–3.94)	0.380
AD (× 10^{-3})	0.85 (0.84–0.88)	0.85 (0.83–0.88)	0.306	0.84 (0.83–0.88)	0.85 (0.84–0.90)	0.115
RD (× 10^{-4})	1.35 (1.28–1.47)	1.29 (1.24–1.37)	0.400	1.49 (1.39–1.62)	1.45 (1.30–1.57)	0.256
Uncinate fasciculus						
FA	0.68 (0.65–0.70)	0.66 (0.64–0.68)	0.272	0.68 (0.66–0.69)	0.65 (0.63–0.69)	0.023*
MD (× 10^{-4})	4.29 (4.20–4.50)	4.10 (4.04–4.36)	0.115	4.15 (4.10–4.26)	4.19 (4.11–4.44)	0.146
AD (× 10^{-3})	0.81 (0.80–0.84)	0.78 (0.75–0.80)	0.007*	0.80 (0.79–0.82)	0.79 (0.77–0.83)	0.182
RD (× 10^{-4})	2.34 (2.16–2.55)	2.32 (2.17–2.53)	0.400	2.28 (2.23–2.34)	2.50 (2.23–2.58)	0.042*
Anterior thalamic radiations						
FA	0.69 (0.67–0.70)	0.68 (0.66–0.69)	0.115	0.69 (0.68–0.70)	0.68 (0.67–0.69)	0.089
MD (× 10^{-4})	3.94 (3.84–3.98)	3.96 (3.74–4.02)	0.420	3.89 (3.87–4.03)	4.03 (3.85–4.18)	0.225
AD (× 10^{-3})	0.77 (0.74–0.77)	0.76 (0.73–0.78)	0.361	0.77 (0.75–0.79)	0.76 (0.75–0.80)	0.380
RD (× 10^{-4})	2.07 (1.99–2.13)	2.17 (2.03–2.25)	0.170	2.10 (1.95–2.19)	2.16 (2.06–2.30)	0.097
Cingulum (cingulate gyrus)						
FA	0.77 (0.76–0.79)	0.80 (0.77–0.81)	0.182	0.74 (0.72–0.76)	0.75 (0.71–0.77)	0.500
MD (× 10^{-4})	3.75 (3.70–3.80)	3.77 (3.64–4.03)	0.306	3.83 (3.68–3.89)	3.80 (3.71–3.88)	0.480
AD (× 10^{-3})	0.83 (0.77–0.84)	0.83 (0.79–0.86)	0.157	0.79 (0.76–0.83)	0.79 (0.74–0.82)	0.361
RD (× 10^{-4})	1.57 (1.49–1.63)	1.57 (1.39–1.63)	0.343	1.78 (1.66–1.81)	1.77 (1.59–1.83)	0.460
Cingulum (angular bundle)						
FA	0.59 (0.57–0.62)	0.59 (0.56–0.65)	0.306	0.61 (0.60–0.63)	0.62 (0.61–0.63)	0.400
MD (× 10^{-4})	4.57 (4.50–4.98)	4.27 (4.10–4.45)	0.007*	4.38 (4.37–4.50)	4.17 (4.09–4.39)	0.017*
AD (× 10^{-3})	0.83 (0.80–0.87)	0.76 (0.72–0.79)	0.011*	0.82 (0.78–0.83)	0.76 (0.73–0.78)	0.005*
RD (× 10^{-4})	2.78 (2.70–2.83)	2.63 (2.37–2.75)	0.035*	2.63 (2.51–2.79)	2.45 (2.39–2.68)	0.089

*Significant at $p < 0.05$.

AD = axial diffusivity, COPD = chronic obstructive pulmonary disease, DTI = diffusion tensor imaging, FA = fractional anisotropy, MD = mean diffusivity, RD = radial diffusivity

Table 3. Partial Correlation with Normalized Hippocampus Volume and K-MMSE Score in All Participants

DTI	Normalized Hippocampus Volume				K-MMSE			
Parameters	Left Hemisphere	*p*-Value	Right Hemisphere	*p*-Value	Left Hemisphere	*p*-Value	Right Hemisphere	*p*-Value
	Forceps major		Forceps minor		Forceps major		Forceps minor	
FA	0.066	0.760	-0.277	0.190	0.093	0.665	0.103	0.631
MD ($\times 10^{-4}$)	-0.266	0.209	0.251	0.238	-0.026	0.902	-0.094	0.661
AD ($\times 10^{-3}$)	-0.174	0.416	-0.173	0.420	0.118	0.584	0.222	0.297
RD ($\times 10^{-4}$)	-0.306	0.146	0.280	0.186	-0.171	0.423	-0.079	0.714
Inferior longitudinal fasciculus								
FA	0.126	0.559	0.025	0.906	0.195	0.362	0.214	0.315
MD ($\times 10^{-4}$)	-0.272	0.199	-0.068	0.752	-0.111	0.605	-0.085	0.693
AD ($\times 10^{-3}$)	-0.057	0.791	-0.078	0.717	0.123	0.568	0.012	0.954
RD ($\times 10^{-4}$)	-0.145	0.498	-0.057	0.790	-0.191	0.373	-0.245	0.248
Superior longitudinal fasciculus (parietal segment)								
FA	-0.055	0.800	-0.011	0.958	0.321	0.126	0.272	0.198
MD ($\times 10^{-4}$)	0.105	0.625	0.166	0.438	-0.623	0.001*	-0.333	0.112
AD ($\times 10^{-3}$)	0.013	0.953	0.203	0.341	-0.327	0.119	-0.381	0.066
RD ($\times 10^{-4}$)	0.071	0.741	0.090	0.676	-0.408	0.048*	-0.339	0.105
Superior longitudinal fasciculus (temporal segment-arcuate)								
FA	0.039	0.858	0.131	0.543	0.094	0.661	-0.262	0.217
MD ($\times 10^{-4}$)	-0.044	0.837	-0.069	0.748	-0.308	0.143	-0.144	0.502
AD ($\times 10^{-3}$)	-0.235	0.270	-0.037	0.863	-0.545	0.006*	-0.439	0.032*
RD ($\times 10^{-4}$)	-0.016	0.941	-0.089	0.678	-0.133	0.535	0.127	0.555
Corticospinal tract								
FA	-0.112	0.602	-0.210	0.325	0.071	0.743	0.045	0.834
MD ($\times 10^{-4}$)	-0.260	0.219	-0.124	0.563	-0.051	0.813	-0.116	0.590
AD ($\times 10^{-3}$)	-0.426	0.058	-0.236	0.266	0.004	0.985	-0.291	0.168
RD ($\times 10^{-4}$)	-0.004	0.986	0.160	0.456	-0.058	0.787	-0.055	0.797
Uncinate fasciculus								
FA	0.152	0.478	0.023	0.914	0.201	0.348	0.423	0.039*
MD ($\times 10^{-4}$)	-0.290	0.170	-0.044	0.838	0.087	0.685	-0.199	0.352
AD ($\times 10^{-3}$)	-0.284	0.179	-0.175	0.414	0.382	0.065	0.236	0.267
RD ($\times 10^{-4}$)	-0.217	0.309	-0.070	0.745	-0.089	0.678	-0.337	0.108
Anterior thalamic radiations								
FA	-0.148	0.490	0.036	0.866	0.267	0.206	0.301	0.152
MD ($\times 10^{-4}$)	-0.298	0.157	-0.145	0.499	-0.269	0.203	-0.234	0.271
AD ($\times 10^{-3}$)	-0.384	0.064	-0.129	0.549	-0.113	0.599	-0.139	0.517
RD ($\times 10^{-4}$)	-0.100	0.643	-0.106	0.621	-0.314	0.135	-0.317	0.131
Cingulum (cingulate gyrus)								
FA	-0.049	0.821	0.105	0.625	-0.285	0.177	-0.178	0.407
MD ($\times 10^{-4}$)	-0.121	0.573	-0.097	0.653	-0.275	0.194	-0.209	0.326
AD ($\times 10^{-3}$)	-0.164	0.444	-0.142	0.507	-0.493	0.014*	-0.309	0.142
RD ($\times 10^{-4}$)	0.009	0.966	0.012	0.956	0.172	0.420	0.041	0.850
Cingulum (angular bundle)								
FA	0.227	0.286	-0.035	0.871	-0.294	0.163	-0.265	0.211
MD ($\times 10^{-4}$)	-0.370	0.075	-0.225	0.291	0.332	0.113	0.282	0.181
AD ($\times 10^{-3}$)	-0.391	0.059	-0.286	0.175	0.285	0.177	0.104	0.629
RD ($\times 10^{-4}$)	-0.243	0.252	0.006	0.978	0.305	0.148	0.431	0.035*

*Significant at $p < 0.05$.

AD = axial diffusivity, DTI = diffusion tensor imaging, FA = fractional anisotropy, K-MMSE = Korean version of the Mini-Mental State Examination, MD = mean diffusivity, RD = radial diffusivity

white matter integrity in COPD patients using TRACULA.

Our study demonstrated an increased number of white matter lesions with altered diffusivity in COPD patients, including the FMAJ, the FMIN, both ILFs, both SLFPs, the left SLFT, both UFs, and both CABs. The K-MMSE scores in COPD patients were significantly lower than those in control participants. These results suggest that alterations of regional white matter integrity are related to cognitive function in COPD patients.

The K-MMSE scores of the participants showed a negative correlation in several white matter tracts, including the left SLFP, both SLFTs, and the left CCG. Of note, the MD and RD of the left SLFP showed a significant negative correlation (MD: r = -0.623, p = 0.001; RD: r = -0.408, p = 0.048) with the K-MMSE score. In addition, COPD patients showed increased MD and RD in the left SLFP relative to healthy controls (MD: p = 0.005, RD: p = 0.035).

Based on the subdivision of the SLF that has been suggested in the literature (32), the SLFP corresponded most closely to the superior longitudinal fasciculus III (SLF III) (1). The SLF III is located in the opercular white matter of the parietal and frontal lobes, extending from the rostral inferior parietal lobule to the ventral part of the premotor and prefrontal cortex. The SLF III links frontal area 44 (the pars opercularis) and the supramarginal gyrus (area 40), which are involved in the articulatory component of language. The connection between the inferior parietal lobule and ventral prefrontal area 46 via this fiber tract has been shown to play a role in working memory (32). The altered diffusivities of the SLFP during COPD may be associated with cognitive changes in COPD patients.

The hippocampus plays a significant role in cognitive function, and a prior study showed that hippocampal atrophy leads to cognitive impairment in COPD patients (5). Structural changes in the hippocampus and altered white matter integrity may cause cognitive dysfunction in COPD patients. Therefore, informative visualization of the relationship between changes in hippocampal volume and white matter integrity is important. In our study, no significant correlation was found between hippocampal volume and diffusion parameters of the white matter tracts, and no volume difference was observed between the control and COPD groups, which is inconsistent with the findings of a previous study (5). Li and Fei (5) proposed that hippocampal atrophy leads to cognitive impairment in COPD, and the degree of atrophy is proportional to arterial oxygen saturation. In this study, we enrolled COPD patients who did not have hypoxemia and had not experienced an acute exacerbation. It is possible that we did not demonstrate the relationship between hippocampal volume changes and COPD in this study. Therefore, further studies with large cohorts should be performed.

The limitations of the study include the small number of patients and the lack of a full assessment of the effect of aging. However, we compared COPD patients with age-matched control individuals. DTI parameters are highly sensitive to motion artifacts, which can be caused by the patient's respiration. To minimize this problem, we recruited only stable nonhypoxemic patients without cardiovascular comorbidities. We also performed visual inspection at the time of MRI acquisition and head motion correction at the time of post-processing.

Interpretation of diffusion parameters is exceedingly complicated, and the specific biological concepts of diffusion metrics are still poorly understood. Although increased MD has been indicated in previous studies as a potential indicator of edema, elevated RD is suggestive of axonal damage or demyelination, and changes in FA describe the degree of directional diffusion organization (33), the manner in which different diffusion metrics are related to one another and define a disease remains to be investigated. Therefore, the precise mechanism by which FA, AD, RD, and MD contribute to characterizing COPD remains to be investigated.

In conclusion, COPD is a systemic disease, and the brain is affected by the disease process. This study demonstrated the alterations of white matter integrity, including those in the SLFP, in COPD patients. This altered white matter integrity may be related to cognitive changes. Hippocampal change, which is important for cognitive function, should be investigated in further studies with larger cohorts.

REFERENCES

1. Yendiki A, Panneck P, Srinivasan P, Stevens A, Zöllei L, Augustinack J, et al. Automated probabilistic reconstruction of white-matter pathways in health and disease using an atlas of the underlying anatomy. *Front Neuroinform* 2011;5:23
2. Song SK, Sun SW, Ramsbottom MJ, Chang C, Russell J, Cross AH. Dysmyelination revealed through MRI as increased radial

(but unchanged axial) diffusion of water. *Neuroimage* 2002;17:1429-1436
3. Wouters EF, Creutzberg EC, Schols AM. Systemic effects in COPD. *Chest* 2002;121(5 Suppl):127S-130S
4. Dodd JW, Chung AW, van den Broek MD, Barrick TR, Charlton RA, Jones PW. Brain structure and function in chronic obstructive pulmonary disease: a multimodal cranial magnetic resonance imaging study. *Am J Respir Crit Care Med* 2012;186:240-245
5. Li J, Fei GH. The unique alterations of hippocampus and cognitive impairment in chronic obstructive pulmonary disease. *Respir Res* 2013;14:140
6. Mori S, Zhang J. Principles of diffusion tensor imaging and its applications to basic neuroscience research. *Neuron* 2006;51:527-539
7. Basser PJ, Mattiello J, LeBihan D. MR diffusion tensor spectroscopy and imaging. *Biophys J* 1994;66:259-267
8. Basser PJ. Inferring microstructural features and the physiological state of tissues from diffusion-weighted images. *NMR Biomed* 1995;8:333-344
9. Lee SH, Coutu JP, Wilkens P, Yendiki A, Rosas HD, Salat DH; Alzheimer's disease Neuroimaging Initiative (ADNI). Tract-based analysis of white matter degeneration in Alzheimer's disease. *Neuroscience* 2015;301:79-89
10. Chong CD, Schwedt TJ. Migraine affects white-matter tract integrity: a diffusion-tensor imaging study. *Cephalalgia* 2015;35:1162-1171
11. Sarica A, Cerasa A, Vasta R, Perrotta P, Valentino P, Mangone G, et al. Tractography in amyotrophic lateral sclerosis using a novel probabilistic tool: a study with tract-based reconstruction compared to voxel-based approach. *J Neurosci Methods* 2014;224:79-87
12. Wozniak JR, Mueller BA, Lim KO, Hemmy LS, Day JW. Tractography reveals diffuse white matter abnormalities in myotonic dystrophy type 1. *J Neurol Sci* 2014;341:73-78
13. Storsve AB, Fjell AM, Yendiki A, Walhovd KB. Longitudinal changes in white matter tract integrity across the adult lifespan and its relation to cortical thinning. *PLoS One* 2016;11:e0156770
14. Pfuhl G, King JA, Geisler D, Roschinski B, Ritschel F, Seidel M, et al. Preserved white matter microstructure in young patients with anorexia nervosa? *Hum Brain Mapp* 2016;37:4069-4083
15. Christodoulou JA, Murtagh J, Cyr A, Perrachione TK, Chang P, Halverson K, et al. Relation of white-matter microstructure to reading ability and disability in beginning readers. *Neuropsychology* 2016 Mar 7 [Epub]. https://doi.org//10.1037/neu0000243
16. Incalzi RA, Gemma A, Marra C, Muzzolon R, Capparella O, Carbonin P. Chronic obstructive pulmonary disease. An original model of cognitive decline. *Am Rev Respir Dis* 1993;148:418-424
17. Dodd JW, Getov SV, Jones PW. Cognitive function in COPD. *Eur Respir J* 2010;35:913-922
18. Ortapamuk H, Naldoken S. Brain perfusion abnormalities in chronic obstructive pulmonary disease: comparison with cognitive impairment. *Ann Nucl Med* 2006;20:99-106
19. Eichenbaum H. Hippocampus: cognitive processes and neural representations that underlie declarative memory. *Neuron* 2004;44:109-120
20. Choi DW, Rothman SM. The role of glutamate neurotoxicity in hypoxic-ischemic neuronal death. *Annu Rev Neurosci* 1990;13:171-182
21. Yendiki A, Koldewyn K, Kakunoori S, Kanwisher N, Fischl B. Spurious group differences due to head motion in a diffusion MRI study. *Neuroimage* 2014;88:79-90
22. Greve DN, Fischl B. Accurate and robust brain image alignment using boundary-based registration. *Neuroimage* 2009;48:63-72
23. Marino-Neto J, Sabbatini RM. A stereotaxic atlas for the telencephalon of the Siamese fighting fish (Betta splendens). *Braz J Med Biol Res* 1988;21:971-986
24. Jenkinson M, Bannister P, Brady M, Smith S. Improved optimization for the robust and accurate linear registration and motion correction of brain images. *Neuroimage* 2002;17:825-841
25. Dale AM, Fischl B, Sereno MI. Cortical surface-based analysis. I. Segmentation and surface reconstruction. *Neuroimage* 1999;9:179-194
26. Fischl B, Sereno MI, Dale AM. Cortical surface-based analysis. II: Inflation, flattening, and a surface-based coordinate system. *Neuroimage* 1999;9:195-207
27. Fischl B, Salat DH, Busa E, Albert M, Dieterich M, Haselgrove C, et al. Whole brain segmentation: automated labeling of

neuroanatomical structures in the human brain. *Neuron* 2002;33:341-355
28. Fischl B, Dale AM. Measuring the thickness of the human cerebral cortex from magnetic resonance images. *Proc Natl Acad Sci U S A* 2000;97:11050-11055
29. Fischl B, Salat DH, van der Kouwe AJ, Makris N, Ségonne F, Quinn BT, et al. Sequence-independent segmentation of magnetic resonance images. *Neuroimage* 2004;23 Suppl 1:S69-S84
30. Behrens TE, Berg HJ, Jbabdi S, Rushworth MF, Woolrich MW. Probabilistic diffusion tractography with multiple fibre orientations: what can we gain? *Neuroimage* 2007;34:144-155
31. Tae WS, Kim SS, Lee KU, Nam EC, Kim KW. Validation of hippocampal volumes measured using a manual method and two automated methods (FreeSurfer and IBASPM) in chronic major depressive disorder. *Neuroradiology* 2008;50:569-581
32. Makris N, Kennedy DN, McInerney S, Sorensen AG, Wang R, Caviness VS Jr, et al. Segmentation of subcomponents within the superior longitudinal fascicle in humans: a quantitative, in vivo, DT-MRI study. *Cereb Cortex* 2005;15:854-869
33. Alexander AL, Lee JE, Lazar M, Field AS. Diffusion tensor imaging of the brain. *Neurotherapeutics* 2007;4:316-329

만성 폐쇄성 폐질환에서 백색질다발통합성 변화: TRActs Constrained by UnderLying Anatomy를 이용한 신경다발 분석

엄미경[1] · 이승환[2,3] · 김우진[4,5] · 조성휘[1] · 윤혜경[1] · 임명남[5] · 편승범[6,7] · 태우석[3,6] · 김삼수[1,3]*

목적: 만성폐쇄폐질환에서 뇌의 구조적 변화와 인지 기능과의 관계를 알아보기 위해 백색질 다발의 통합성 변화와 해마의 부피 변화를 알아보고자 하였다.

대상과 방법: 13명의 저산소혈증이 없는 만성폐쇄폐질환이 있는 남자 환자와 13명의 동일한 연령대의 남성을 대상으로 확산텐서영상과 3D-T1 강조영상을 얻었다. 종합적 확률론적 신경다발 영상기법을 이용하여 18개 신경다발 영상을 얻어 비교하였다. 또한 신경다발의 확산인자와 해마의 부피변화와의 연관성을 분석하였다.

결과: 11개 신경다발의 확산인자에서 두 군 간 유의한 차이를 보였다($p < 0.05$). 일반화시킨 해마의 부피와 확산인자는 유의한 연관성을 보이지 않았다. 한국형 간이정신상태검사 점수와 여섯 개 신경다발의 확산인자에서 유의한 연관성을 보였다($p < 0.05$). 그중에서 왼쪽 위세로다발이 음의상관관계를 보였다(mean diffusivity: $r = -0.623$, $p = 0.001$; radial diffusivity: $r = -0.408$, $p = 0.048$).

결론: 백색질 신경다발 통합성 변화는 만성폐쇄성폐질환 환자에서 위세로다발을 포함한 여러 신경다발에서 관찰되었으며, 인지변화와 연관이 있었다. 해마의 부피 변화와의 연관성을 밝히기 위해서는 추가적인 연구가 필요하다.

강원대학교 의학전문대학원 강원대학교병원 [1]영상의학과, [2]신경과, [4]내과,
강원대학교 의학전문대학원 강원대학교병원 [3]뇌영상연구소, [5]환경보건센터,
고려대학교 의과대학 고려대학교 안암병원 [6]융합뇌신경연구센터, [7]재활의학과